



AFM and SEM-FEG study on fundamental mechanisms leading to fatigue crack initiation



J. Man^{a,*}, M. Valtr^b, M. Petreac^{a,1}, J. Dluhoš^c, I. Kuběna^a, K. Obrtlík^a, J. Polák^{a,d}

^a Institute of Physics of Materials ASCR, Žitkova 22, 616 62 Brno, Czech Republic

^b Czech Metrology Institute, Okružní 31, 638 00 Brno, Czech Republic

^c TESCAN, a.s., Libušina tř. 21, 623 00 Brno, Czech Republic

^d CEITEC IPM, Institute of Physics of Materials ASCR, Žitkova 22, 616 62 Brno, Czech Republic

ARTICLE INFO

Article history:

Received 30 September 2013

Received in revised form 27 February 2014

Accepted 24 September 2014

Available online 2 October 2014

Keywords:

Fatigue crack initiation

316L austenitic stainless steel

Atomic force microscopy (AFM)

Extrusion

Intrusion

ABSTRACT

Early stages of surface relief evolution of persistent slip markings (PSMs) in polycrystalline 316L austenitic stainless steel cycled with constant plastic strain amplitude at 93, 173 and 573 K were studied using atomic force microscopy (AFM) and high-resolution scanning electron microscopy (SEM-FEG). Qualitative and quantitative data on the morphology of PSMs, occurrence of extrusions and intrusions and the kinetics of extrusion growth are reported for all temperatures. PSMs start in all cases as surface extrusions which are later accompanied by formation of intrusions. This finding is discussed with respect to the point defect formation within areas of localized cyclic slip and primarily to their mobility at different temperatures. Consequences of migration of respective point defects for surface relief formation and the conditions for creation of fatigue crack embryos, i.e. sharp intrusions are highlighted.

© 2014 Elsevier Ltd. All rights reserved.

1. Introduction

The knowledge of fatigue crack initiation mechanisms is one of the fundamental but, unfortunately, still only partially answered questions in the study of fatigue damage of materials. The damaging process starts preferentially at the sites of cyclic strain localization, now usually called persistent slip bands (PSBs) and results in the formation of sharp surface slip markings (called persistent slip markings – PSMs). PSMs consist of local elevations and depressions of the surface, known as extrusions and intrusions, which develop on the initially flat surface at emerging PSBs, for a review see e.g. [1–7]. Although it is generally accepted that PSMs represent incipient fatigue crack sites, the detailed review on this topic showed that the exact mechanism of fatigue crack nucleation has not been yet clarified completely [8]. Some other more recent considerations and diverse views on mechanisms and processes leading to fatigue crack initiation can be found elsewhere [9–17]. Since some theoretical models highlight an important role of *point defects* in the process of fatigue crack initiation and predict temperature dependence of surface relief evolution (see e.g. [18–21]), it is desirable and crucial for their verification to obtain detailed

experimental data on the PSM formation not only at room temperature but also at elevated and particularly at depressed temperatures.

The surface relief topography of PSMs and its evolution have been amply studied by various experimental techniques in specimens fatigued at room temperature, see e.g. [1–5,7,10,11,13,22–29]. Although the presence of PSMs has been evidenced down to 4.2 K more than fifty years ago [30,31], detailed experimental data on surface relief evolution for elevated and especially for depressed temperatures are rare so far. Fatigue crack initiation at 298, 77 and 4.2 K was studied by Kwon et al. both in single- [32] and polycrystalline [33] copper. Three characteristic morphologies of macro-PSMs in copper single crystals fatigued in the temperature range 4.2–350 K were revealed using sharp corner polishing technique by Basinski and Basinski [34]. Morphology and growth of extrusions in single- [35] and polycrystalline [35,36] copper at 107, 298 and 473 K was quantitatively documented using the contamination line technique in scanning electron microscopy (SEM) by Mughrabi and his co-workers [10]. Available experimental data clearly show that morphology and profiles of PSMs and the extrusion growth are temperature dependent but until now no systematic investigations of the temperature dependence are available.

This work represents a continuation and expansion of our experimental studies on the fundamental mechanisms leading to

* Corresponding author.

E-mail address: man@ipm.cz (J. Man).

¹ Present address: TESCAN, a.s., Libušina tř. 21, 623 00 Brno, Czech Republic.

Table 1
Chemical composition (in wt.%) of 316L steel.

C	Si	Mn	P	S	N ^a	O ^a	Cr	Ni	Mo	Fe
0.018	0.42	1.68	0.015	0.001	0.071	0.003	17.6	13.8	2.6	Rest

^a Supplementary determination by gas fusion method in addition to chemical composition guaranteed by Uddeholm.

fatigue crack initiation using modern microscopic techniques – atomic force microscopy (AFM) and high-resolution SEM equipped with field emission gun electron source (SEM-FEG). Detailed experimental data obtained for austenitic 316L steel so far in room temperature cycling (direct specimen observation and plastic replica) [23,37] are in the present work extended to cycling at depressed and elevated temperatures. Preliminary results on this subject have been already published elsewhere [38]. In this paper qualitative and quantitative data on the morphology of PSMs and extrusion growth obtained are discussed in relation to the predictions of the recent *point defect* models of surface relief formation and fatigue crack initiation.

2. Experimental

Specimens were machined from a 25 mm thick plate of austenitic 316L stainless steel (Uddeholm, Sweden) with axis parallel to the rolling direction. The chemical composition of the steel is given in Table 1. The heat treatment, consisting of solution annealing at 1080 °C and water quenching, resulted in an average grain size of 39 μm (found using linear intercept method without counting twin boundaries).

Cylindrical specimens with threaded ends having gauge diameter and length of 8 and 12 mm, respectively, were adopted for depressed temperatures. Cylindrical button-end specimens of 6 mm in diameter and 15 mm in gauge length were used for fatigue tests at elevated temperatures. To facilitate the surface relief observation a shallow notch was produced in both specimen geometries by grinding a cylindrical surface 60 mm in diameter with the axis perpendicular to the specimen axis to a depth of 0.4 mm. After machining the specimens were annealed at 600 °C for 1 h in vacuum and the notch area was polished mechanically and electrochemically. For easier orientation on the specimen surface fine circular marks 400 μm in diameter were engraved on the central part of the polished notch.

Fatigue tests at 93, 173 and 573 K were carried out in a MTS computer-controlled servohydraulic testing machine in symmetrical push–pull cycle ($R_\epsilon = -1$) in strain control. Plastic strain amplitude $\epsilon_{ap} = 1 \times 10^{-3}$, derived from the half-width of the hysteresis loop, and the total strain rate $\dot{\epsilon} = 1.5 \times 10^{-3} \text{ s}^{-1}$ were kept constant during the tests at all temperatures. Details concerning the cryostat and temperature control in low-temperature tests are given elsewhere [39]. Elevated temperature cyclic straining has been periodically interrupted for surface relief study. Another methodology was, however, applied for the study of surface relief at depressed temperatures. In order to avoid room-temperature warming up periods during cycling of an individual specimen and thus prevent their possible effect on point defect migration, several specimens were cycled at 93 and 173 K to different early stages of fatigue life. In both ways experimental data on surface relief evolution could be obtained. Deformation history of all specimens is apparent from Table 2.

The detailed study of surface topography and its evolution on the specimen surface was performed using AFM (Accurex III, Topometrix) directly on the metallic specimen surface and for selected specimens also on its inverse copy obtained using plastic replica (for detailed description of replication procedure see [23]).

AFM in contact imaging mode in air was used to obtain constant-force topographic images. A V-shaped silicon nitride cantilever with a sharpened pyramidal tip having the radius of curvature of 20 nm and the vertex angle 36° was applied. The basic scan size $100 \times 100 \mu\text{m}^2$ with resolution 400×400 data points was used for an overall documentation of slip distribution. For the detection of intrusions and quantitative analysis of extrusion growth, areas of $15 \times 15 \mu\text{m}^2$ or smaller, with 500×500 data points were captured. For better visualization of intrusions all plastic replica micrographs are displayed in non-inverted format. Surfaces of fatigued specimens were additionally documented by high-resolution SEM-FEG LYRA I or MIRA II from Tescan Co.

3. Results

3.1. Surface relief at depressed temperatures

Surface observations of 316L steel fatigued at 173 K with plastic strain amplitude 1×10^{-3} showed very early the localization of cyclic slip manifested by the appearance of distinct PSMs. Already after 500 cycles fine PSMs were detected in about 15% of grains. With increasing number of cycles PSMs intensified and the fraction of grains with PSMs grew gradually. At 4500 cycles more than 75% of the grains were covered by PSMs and at 9000 cycles practically all grains were affected by cyclic slip localization. Cyclic plastic strain in the grains is generally accommodated by PSBs appertaining to one slip system. Cyclic straining produces PSMs whose spacing was approximately constant at different stages of fatigue life (see Table 2).

General features of PSM morphology at 173 K were found to be similar to that obtained at room temperature [23]. PSMs start as surface extrusions which are later accompanied by thinner parallel intrusions. Intrusions running parallel along ribbon-like extrusions have been revealed by SEM-FEG already after 500 cycles (Fig. 1). The intrusions develop later than extrusions and often only locally along extrusions (see a less developed PSM in Fig. 1a). In later stages the surface relief does not change significantly: both mature PSMs consisting of extrusions and intrusions and younger, less developed PSMs consisting only of extrusions can be found (see two thin PSMs close to the upper right corner in Fig. 1b). In some cases the alternations of tongue-like extrusions and intrusions within an individual PSM are also detected – see Fig. 1b. Note that on both SEM-FEG micrographs, due to the inclination of the active slip plane to the specimen surface, intrusions are unfailingly detectable only along the right side of extrusions. More specifically and in agreement with the nomenclature introduced earlier [18] it is the side “A” of an extrusion where the emerging active slip plane is inclined to the surface at an obtuse angle.

Fig. 2 shows finer details of PSM topography obtained by AFM that explicitly documents the three-dimensional character of PSMs. While intrusions accompanying extrusions could be revealed by AFM on specimen surface only for less developed PSMs in early stages of fatigue life (see Fig. 2a), the adoption of replica technique proved that in later stages of fatigue life the majority of PSMs consists of extrusions and intrusions running parallel along one (Fig. 2b) or both (Fig. 2c) of their sides. Intrusions are often developed only locally; their depth fluctuates along PSMs.

Table 2
Fatigue test conditions and PSM characteristics.

Specimen No.	Temperature (K)	Cycles	Average PSM spacing (μm)	Extrusion height (nm)	
				Average	Maximum
UD 371	173	500	4.8 ± 1.1	32 ± 30	140–170
UD 372	173	1000	4.5 ± 1.4	72 ± 57	280–320
UD 373	173	2000	4.6 ± 0.9	115 ± 64	280–320
UD 374	173	4500	4.2 ± 0.6	168 ± 83	420–470
UD 450	173	9000	4.5 ± 1.2	221 ± 95	520–670
UD 379	93	1000	1.5 ± 0.3	17 ± 9	30–45
UD 381	93	2000	1.2 ± 0.4	25 ± 9	40–80
UD 382	93	4500	1.2 ± 0.4	27 ± 10	40–70
UD 383	93	9000	1.2 ± 0.7	27 ± 11	40–60
UD 424	573	100	5.6 ± 1.5	71 ± 35	180–230
UD 424	573	250	3.8 ± 1.5	131 ± 73	290–380

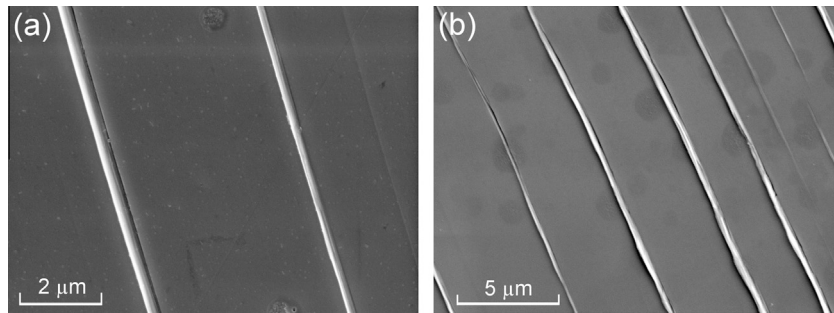


Fig. 1. SEM-FEG micrographs of surface relief in 316L steel fatigued at 173 K with $\epsilon_{ap} = 1 \times 10^{-3}$ to different number of cycles. (a) $N = 500$ (UD371); and (b) $N = 2000$ (UD373). Stress axis is horizontal in both micrographs.

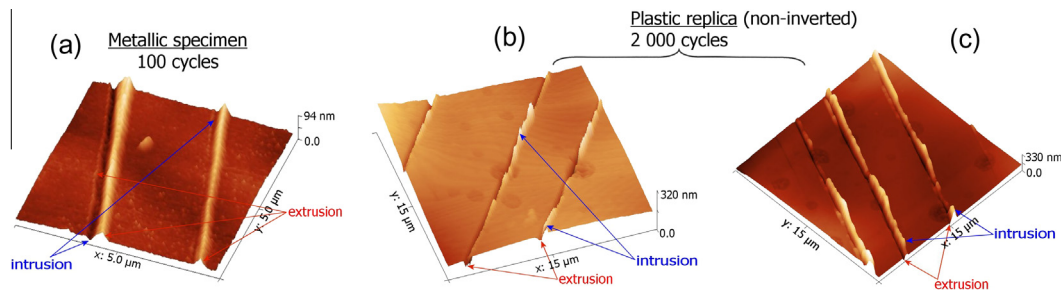


Fig. 2. Three-dimensional AFM images of extrusions and intrusions in 316L steel fatigued at 173 K with $\epsilon_{ap} = 1 \times 10^{-3}$ to different number of cycles.

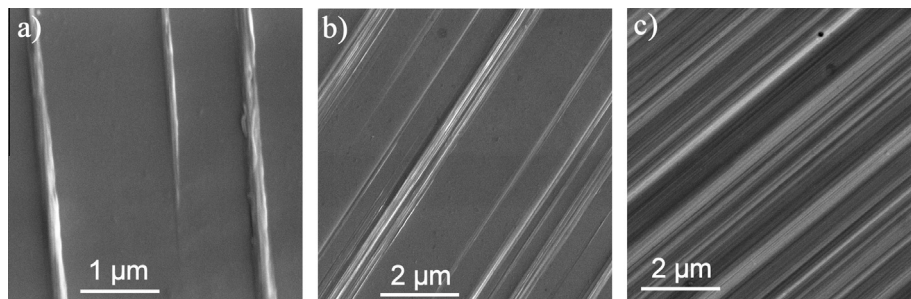


Fig. 3. Surface relief topography within grains of 316L steel fatigued at 93 K with $\epsilon_{ap} = 1 \times 10^{-3}$ for 9000 cycles (SEM-FEG).

Great variability of surface relief topography found at 93 K witnesses a more complicated slip behavior as well as presumably the participation of different types of point defects in formation of PSMs (see Section 4) in 316L steel fatigued at this temperature. Several characteristic features of surface topography were revealed as documented in detail in Figs. 3–6 obtained by SEM-FEG and AFM.

Fig. 3a–c document appreciable variability of the surface relief developed in individual grains after 9000 cycles. Fig. 3a shows three individual PSMs consisting of extrusions whose width is around 200 nm. Hilly nature of thin extrusions is clearly visible from AFM image in Fig. 4a. Surface profile (section A in Fig. 4c) reveals the presence of small slip steps accompanying extrusions and reveals also very small intrusions accompanying only two

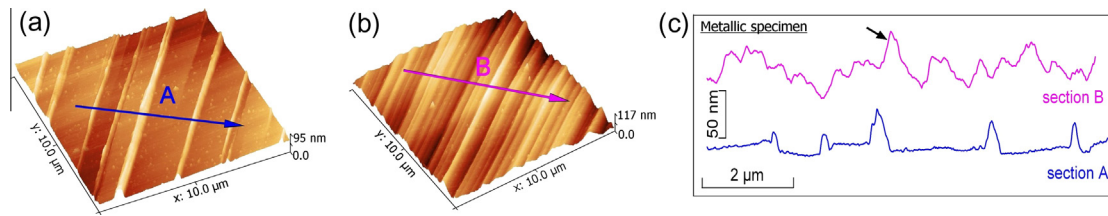


Fig. 4. Characteristic forms of surface relief topography and corresponding profiles in 316L steel fatigued at 93 K with $\epsilon_{ap} = 1 \times 10^{-3}$ for 9000 cycles. AFM, metallic specimen surface.

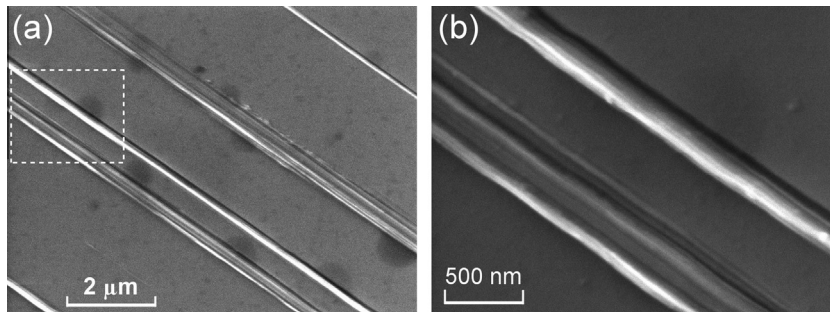


Fig. 5. Surface relief within a grain of 316L steel fatigued at 93 K with $\epsilon_{ap} = 1 \times 10^{-3}$ for 4500 cycles (UD382) as obtained by SEM-FEG. (a) Overview micrograph at lower magnification, and (b) detail of PSMs taken from area denoted in (a). Stress axis is horizontal.

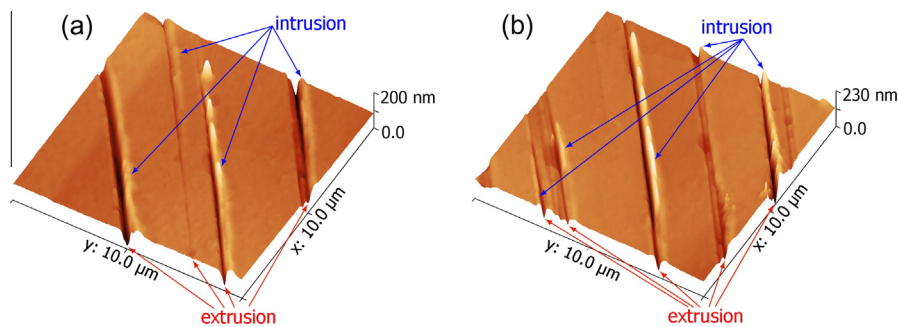


Fig. 6. Details of intrusions and extrusions in 316L steel fatigued at 93 K with $\epsilon_{ap} = 1 \times 10^{-3}$ for 4500 cycles. AFM, plastic replica (non-inverted).

extrusions in Fig. 4a. Both features are similar to those observed earlier in room temperature cycling [23,37]. The extrusion height is typically only 20–35 nm after 9000 cycles. The average spacing of thin PSMs is smaller in comparison with those produced at 173 K (see Table 2). Fig. 3b shows both very thin and also wide PSMs (up to 1 μm) separated by original flat surface. Wide PSMs consist of several closely spaced extrusions.

Since extrusions are generally finer and represent the most striking feature of PSMs, only very detailed inspection by SEM-FEG at high magnification (Fig. 5) and/or the adoption of replica technique in AFM study (Fig. 6) can reveal the presence of intrusions and thus find the true morphology of PSMs. SEM-FEG micrograph taken at very high magnification (see the detail in Fig. 5b which is indicated in Fig. 5a) as well as AFM images of plastic replicas in Fig. 6 show that both individual PSMs and wider PSMs already after 4500 cycles at 93 K consist of both extrusions and intrusions. Intrusions could be developed only locally and their depth, similarly to 173 K, fluctuates along PSMs (see Fig. 6). Due to the limitations of AFM in observation of the true surface relief topography [37,40] the width of PSMs cannot be determined from Fig. 6. Only SEM-FEG micrographs of specimen surface taken with high resolution can be used for assessment of intrusion and extrusion width. Limited data obtained so far indicate that the difference

in the intrusion and extrusion thickness at this temperature is much smaller than at temperatures above 173 K (see Fig. 5b).

Besides distinct individual PSMs and wide PSMs, clearly separated by a smooth surface area corresponding to the matrix, we have found fine slip markings with peak-to-valley topography covering homogeneously selected parts of surface grains and later completely the whole surface of some grains. This specific form of cyclic slip localization in 316L steel fatigued at 93 K is documented in Fig. 3c and in three dimensions in Fig. 4b. The mean height of peak-to-valley profile can differ from grain to grain but its typical value is about 30–40 nm (see section B in Fig. 4c). The serrated profile (section B in Fig. 4c) does not mostly allow to distinguish individual extrusions or intrusions. Since this profile covers at large number of cycles the whole grain it is even difficult to interpret the profile as extrusions and intrusions. It is similar to profiles developed in fatigued Cu–30 wt% Zn alloys e.g. [41,42] and can arise also as a result of random slip or timely limited persistent slip. Nevertheless a small hilly extrusion could be sometimes located within peak-to-valley structure (see small extrusion in the middle of section B in Fig. 4c marked with arrow) which indicates the persistency of cyclic slip at this location.

The last specific surface feature detected in 316L only in specimens cycled at the lowest temperature represents specific surface

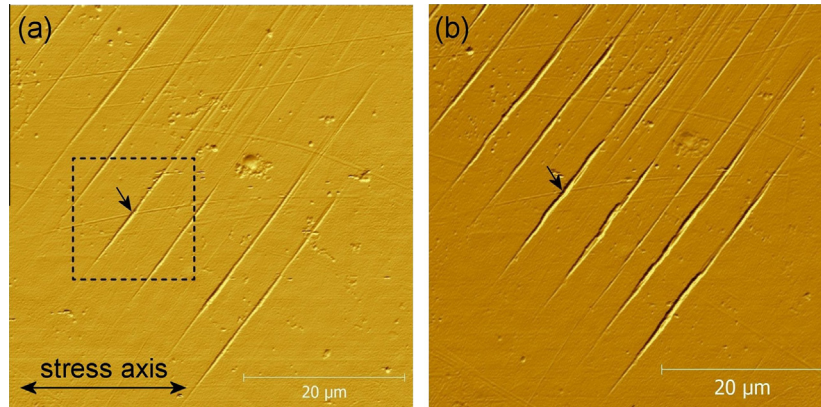


Fig. 7. Surface relief within a grain of 316L steel fatigued with $\epsilon_{ap} = 1 \times 10^{-3}$ at 573 K as obtained by AFM after (a) 100, and (b) 250 cycles. AFM micrographs are displayed in shadowed format.

relief connected with the presence of deformation induced martensite. This topic is however beyond the scope of the present paper and its description can be found elsewhere [38].

3.2. Surface relief at elevated temperature

Characteristic features of the early evolution of overall slip activity in 316L steel fatigued at 573 K shows Fig. 7. PSMs were found in specimens cycled at this temperature for 100 cycles but only in a few grains. They do not cover evenly the whole surface grain. PSMs typically develop locally along the intersection of PSBs with the specimen surface (see Fig. 7a). Average PSM spacing is slightly higher in comparison with that found at 173 K (see Table 2). With increasing number of cycles the number of grains covered by PSMs gradually increases and at the same time PSMs developed earlier, intensify considerably. In addition to the heightening and lengthening of existing PSMs some new ones appear after 250 cycles (cf. Fig. 7a and b) which results in the decrease of average PSM spacing (see Table 2).

Details of PSM topography from the area denoted in Fig. 7a show three-dimensional AFM images in Fig. 8. Direct observations of specimen surface showed that PSMs consist of ribbon-like extrusions the height of which slightly fluctuates along their length (see Fig. 8a and b). The average and the maximum extrusion height evaluated in several grains by AFM increases considerably with increasing number of cycles; their values are listed in Table 2. The width of some PSMs also locally increases via local widening of PSBs (cf. Fig. 8a and b). A very important feature of surface relief topography in cycling at temperature 573 K yields plastic replica technique (see Fig. 8c). Fig. 8c shows the identical area of the grain as that in Fig. 8a. In non-inverted image of plastic replica parallel intrusions accompanying locally extrusions are already present in 316L steel

even in this very early stage of fatigue life. Similarly to intrusions found in room and low temperature cyclic straining their depth is not constant but fluctuates along PSMs (see Fig. 8c). The maximum depth of intrusions found from AFM observations on replicas taken at $N = 100$ cycles in 7 grains was 160–190 nm.

3.3. Growth of extrusions at depressed and elevated temperatures

Quantitative data on the growth of extrusions were obtained for all temperatures from the profiles of individual PSMs in selected sections evaluated from AFM micrograph of the specimen surface. In agreement with our previous studies on surface relief and its evolution in 316L [17,33,24] the sections were taken perpendicular to the surface and to the direction of the PSMs. The height of an extrusion was evaluated in five different sections. The height of each extrusion represents the average of these five values. About 10 grains and more than 100 PSMs were evaluated for specimens cycled at 173 and 93 K to different stages of fatigue life. In the case of surface relief study at 573 K during intermittent cycling more than 100 PSMs in 10 grains were evaluated only at 250 cycles; at 100 cycles the number of grains containing PSMs was limited to 5. The results of statistical treatment of the average and maximum extrusion heights at three different temperatures are listed in Table 2. The kinetics of extrusion growth is presented in Fig. 9. In spite of a great scatter of experimental data systematic extrusion growth with the number of cycles is apparent at 173 K and 573 K while at 93 K the initial growth is followed by saturation of the average extrusion height. The extrusion growth rate at 173 K is highest during the initial period and decreases with the number of cycles (see Fig. 9). The initial rate of the extrusion growth at temperature 573 K is around 6×10^{-10} m/cycle and at temperature 173 K it is around 7×10^{-11} m/cycle, i.e. more than an order of

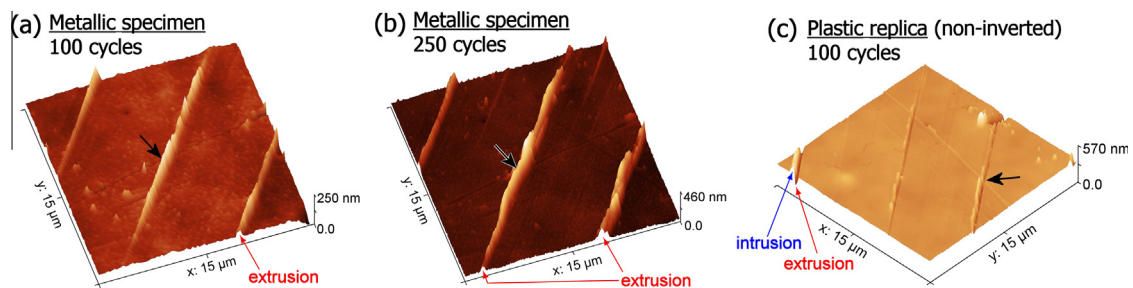


Fig. 8. Details of PSMs obtained by AFM in area denoted in Fig. 7a using direct observation of specimen surface (a and b) and using plastic replica, (c) after different number of cycles. Small black arrows indicate the same position on all AFM micrographs. 316L steel, $\epsilon_{ap} = 1 \times 10^{-3}$, 573 K.

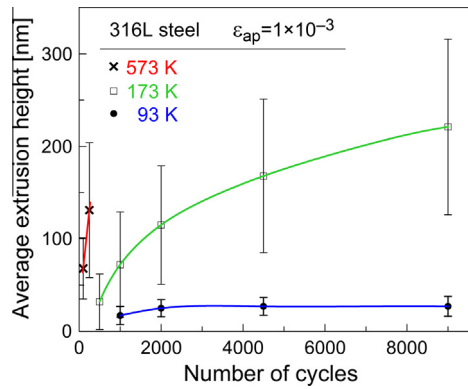


Fig. 9. Growth of extrusions in 316L steel fatigued at different temperatures.

magnitude lower than that at 573 K. Extrusion growth kinetics at the lowest temperature of 93 K differs from that at 173 K and 573 K but also from that at room temperature [23,37,40]. Average initial extrusion rate at 93 K is much smaller and with continuing cycling drops to zero and the saturated extrusion height is very small (see Fig. 9 and Table 2).

4. Discussion

Experimental study of the surface relief evolution produced in austenitic 316L steel by constant plastic strain amplitude cyclic loading at two depressed temperatures and one elevated temperature, simultaneously with previous room temperature data [23,37] yields new information about the temperature dependence of the shape and kinetics of surface relief formation of a polycrystalline material. The principal experimental findings can be summarized as follows:

- (i) PSMs produced at all temperatures start as ribbon-like extrusions that grow and later are accompanied by parallel intrusions. Intrusions can appear on one or on both sides of the extrusion often only along partial segments of an extrusion. The depth of intrusions is variable.
- (ii) Appreciable variability in the change of surface relief exists at each temperature.
- (iii) The extrusion growth rate is temperature dependent. Initial growth rate strongly increases with temperature. At 93 K the growth rate drops to zero and extrusion height saturates or even has a tendency to decrease.
- (iv) Average spacing of PSMs also increases with increasing temperature.
- (v) Contrary to room and elevated temperature where the width of extrusion is much larger than the width of intrusions, at the lowest temperature (93 K) their width is approximately the same.

The experimental finding on the temperature dependence of the surface relief can be confronted with the predictions of the existing models of surface relief formation and fatigue crack initiation. Though there are numerous models of fatigue crack initiation (see e.g. [1,4,5,7,8,11,12,16–21]) only a few are based on the real dislocation structure of the PSBs. PSBs are sites of cyclic slip localization and are, as generally agreed [1–13,16,17], the source of the pronounced surface relief in the form of PSMs. PSMs arise in locations where PSBs egress on the surface and fatigue cracks initiate there.

The first physically based model of fatigue crack initiation was model proposed by Essmann et al. [18] (EGM model) (see also Ref. [1,3,10,12]). It is based on the knowledge of the dislocation

arrangement in the PSB [43,44] and resistivity measurement of point defect production in cyclic loading [45,46]. In EGM model not only dislocation motion is considered but also dislocation interactions, namely the annihilation of edge dislocations which leads to point defect formation (preferentially vacancies). The production of vacancies combined with irreversible slip processes results in the elongation of the PSB and formation of a *static extrusion*. The height of this static extrusion is proportional to the non-equilibrium concentration of vacancies produced in the PSB due to localized cyclic straining. As a result of extrusions type I stress raisers arise and random slip in PSB leads to the production of type II stress raisers. Fatigue cracks arise due to stress concentration on both types of raisers.

Most important objection against EGM model is the fact that extrusions are produced also at temperatures at which vacancies are mobile and disappear from the PSB by migration to edge dislocations. Provided vacancies are mobile at a particular temperature no static extrusion can arise. The isochronal annealing curves of single and polycrystalline copper cycled at low temperature [47,48] clearly show point defect annealing stages below room temperature. In 316L steel (see Section 3) it was found that the extrusion growth is highest at elevated temperature (573 K) and lowest at low temperature (93 K). It can be thus hardly explained as static extrusion growth.

Detailed experimental observations of PSMs produced by cyclic loading in copper single crystals [49] and annealing studies of point defect produced in cyclic loading led Polák [19] to propose substantial modification of the EGM model. In Polák's model the static extrusion plays only a minor role but surface relief is formed due to steady production of point defects in PSB and their simultaneous migration to the edge dislocations in the matrix. In constant strain rate and constant strain amplitude cyclic loading in each cycle vacancies (or interstitials) are produced in PSB and fraction of them migrates to the matrix and is annihilated there. This process leads to the redistribution of matter between PSB and thin sheets of neighbor matrix. As a result increasing internal compression stresses are generated in the PSB and increasing internal tensile stresses are generated in the thin sheets of the matrix close to the PSB/matrix interface. These internal stresses are plastically relaxed and from the PSB an extrusion grows and at both PSB/matrix interfaces intrusions arise.

Quantitative treatment of the point defect production and migration has been performed by Polák and Sauzay [20] in evaluating the shape of an extrusion assuming PSB matrix boundary is a perfect sink for vacancies. Recently Polák and Man [21] provided the complete quantitative solution of the migration and annihilation of vacancies produced in PSB and derived the shape of the central extrusion and two parallel intrusions provided vacancy type defect is produced and migrates at a given temperature. Our experimental data could be thus used for checking the validity of the predictions of this model.

Unfortunately the data on point defect migration in 316L steel are very limited. Dimitrov and Dimitrov [50] found in irradiated Fe–Cr–Ni austenitic alloy pronounced point defect annealing stage starting at 20–200 K with activation energies in the range 0.2–0.5 eV. Though experiments on point defect production and migration in 316L steel after cyclic plastic straining are not available it is apparent that point defects are mobile at temperatures starting already at very low temperature. Therefore, the mechanisms leading to the transfer of matter between the PSB and the matrix based on point defect migration can be operative at all investigated temperatures.

Majority of experimental findings at temperature 173 K and above (see Section 3 and summary above) are in reasonable agreement with the predictions of the Polák's model. Important achievement of the model is the explanation of the delayed

appearance of the intrusion (or intrusions) parallel to the central extrusion. The reason for the delayed appearance of the intrusions or even for no intrusion at all is the higher yield stress of the matrix relative to the yield stress of the PSB [21]. The variability of the dislocation arrangement in the matrix close to the PSB/matrix interface (see e.g. [43,44,51]), which represent the sinks for point defects, results in the variability of the intrusions accompanying extrusions.

Most important agreement between the model and present experimental observations is the predicted shape and the small width of the intrusion relative to the width of the extrusion. The true shape of a thin intrusion before the fatigue crack starts from its tip is difficult to assess experimentally. The best method to acquire the shape of PSM are the sharp polishing technique used by Basinski and Basinski [4,34] and Ma and Laird [52] and the FIB cuts used recently [17,25,26,28]. Simultaneously with the present data they indicate the presence of sharp intrusions from which the cracks could initiate.

The kinetics of extrusion growth, namely the strong temperature dependence of the extrusion rate is also compatible with the Polák's model. The growth rate of the extrusion in the center r_{Ec} was evaluated by Polák and Man [21]

$$r_{Ec} = \frac{pl}{\cosh(aw/2) + \frac{a}{\sqrt{\rho_e}} \sinh(aw/2)} \quad (1)$$

where p is the production rate of a specific point defect, l is the depth of the surface grain in the direction of the Burgers vector, w is the width of the PSB, ρ_e the density of edge dislocations in the matrix which serve as sinks for point defects and $a = \sqrt{A/\tau D}$ is a kinetic parameter which depends on the annihilation coefficient A of point defects during cyclic plastic straining, on the period of cycling τ and on the diffusion coefficient D of the migrating point defect. Since diffusion coefficient rapidly increases with temperature also extrusion rate evaluated according to Eq. (1) increases until it reaches the saturation value at temperature where all point defects generated during cyclic plastic straining in PSB are able to be transferred to the matrix and contribute to the growth of both extrusion and parallel intrusions. Predicted temperature dependence of the extrusion growth rates are calculated elsewhere [21]. They depend critically on the activation energy of the migrating point defect.

The situation at the lowest temperature (93 K) is different from that at higher temperatures. The extrusion height reaches very soon its saturated value which is very low. It corresponds to the height of the "static" extrusion in the EGM model. However the presence of both extrusions and intrusions in the PSM produced at temperature 93 K indicates the participation of both vacancy as well as interstitial types of defects in their formation. The possible participation of interstitial type defects in the formation of surface relief of materials cycled at low temperature has been recently proposed by Polák and Man [53]. More precise prediction on the shape and kinetics of PSMs formation can be made only when the production rates and migration properties of individual defect at a specific temperature are assessed.

5. Conclusions

An AFM and SEM-FEG study of the early stages of surface relief evolution in polycrystalline 316L austenitic stainless steel cycled with constant plastic strain amplitude at depressed and elevated temperatures allows drawing the following conclusions:

- (i) Cyclic plastic straining at all investigated temperatures is localized into PSBs which produce distinct PSMs consisting of extrusions and intrusions.
- (ii) PSMs exhibit great variability but characteristic feature at temperatures 173 K and above is the presence of central extrusion accompanied on some segments by thin intrusions.
- (iii) Growth of extrusions is temperature dependent. At 93 K rapidly small extrusion height is achieved with a tendency to shrinkage in further cycling. The extrusion growth rate increases rapidly with increasing temperature.
- (iv) Experimental data on the temperature dependence of the extrusion growth and shape of PSMs are compatible with the recent formulation of Polák's model of surface relief formation and crack initiation.

Acknowledgements

Authors are indebted to Dr. P. Doležal from Brno University of Technology for the supplementary chemical analysis of 316L steel. The work was realized in CEITEC with research infrastructure supported by the project CZ.1.05/1.1.00/02.0068 financed from European Regional Development Fund. Financial support of this work by the research project RVO 68181723 and by the Grants Nos. P108/10/2371 and 13-23652S from the Czech Science Foundation is gratefully acknowledged.

References

- [1] Mughrabi H, Wang R, Differt K, Essmann U. Fatigue crack initiation by cyclic slip irreversibilities in high-cycle fatigue. In: Lankford J, Davidson DL, Morris WL, Wei RP, editors. Fatigue mechanisms: advances in quantitative measurement of physical damage, ASTM STP 811. Philadelphia: American Society for Testing and Materials; 1983. p. 5–45.
- [2] Neumann P. Fatigue. In: Cahn RW, Haasen P, editors. Physical metallurgy, Part 2. Amsterdam: Elsevier Science; 1983. p. 1553–94.
- [3] Mughrabi H. Dislocations in fatigue. Dislocations and properties of real materials, Book No. 323. London: The Institute of Metals; 2000. p. 244–62.
- [4] Basinski ZS, Basinski SJ. Prog Mater Sci 1992;36:89–148.
- [5] Laird C. Fatigue. In: Cahn RW, Haasen P, editors. Physical metallurgy, 4th ed., vol. 3. Amsterdam: Elsevier Science; 1996. p. 2293–397.
- [6] Lukáš P. Fatigue crack initiation mechanisms. In: Buschow KHJ, Cahn RW, Flemings MC, Ilshner B, Kramer EJ, Mahajan S, editors. Encyclopedia of materials: science and technology, vol. 3. Oxford: Elsevier Science; 2001. p. 2884–94.
- [7] Polák J. Cyclic deformation, crack initiation, and low-cycle fatigue. In: Milne I, Ritchie RO, Karihallo B, editors. Comprehensive structural integrity, vol. 4. Amsterdam: Elsevier; 2003. p. 1–39.
- [8] Man J, Obrtlík K, Polák J. Extrusions and intrusions in fatigued metals. Part 1. State of the art and history. Phil Mag 2009;89:1295–336.
- [9] Risbet M, Feugas X. Some comments about fatigue crack initiation in relation to cyclic slip irreversibility. Eng Fract Mech 2008;75:3511–9.
- [10] Mughrabi H. Cyclic slip irreversibilities and the evolution of fatigue damage. Metall Mater Trans A 2009;40:1257–79.
- [11] Chan KS, Tian JW, Yang B, Liaw PK. Evolution of slip morphology and fatigue crack initiation in surface grains of Ni200. Metall Mater Trans A 2009;40:2545–56.
- [12] Mughrabi H. Fatigue, an everlasting material problem – still an vogue. Proc Eng 2010;2:3–26.
- [13] Ho HS, Risbet M, Feugas X, Moulin G. The effect of grain size on the localization of plastic deformation in shear bands. Scripta Mater 2011;65:998–1001.
- [14] Brinckmann S, Sivanesapillai R, Hartmaier A. On the formation of vacancies by edge dislocation dipole annihilation in fatigued copper. Int J Fatigue 2011;33:1369–75.
- [15] Sangid MD, Maier HJ, Sehitoglu H. A physically based fatigue model for prediction of crack initiation from persistent slip bands in polycrystals. Acta Mater 2011;59:328–41.
- [16] Sangid MD. The physics of fatigue crack initiation. Int J Fatigue 2012;57:58–72.
- [17] Brown LM. Cracks and extrusions by persistent slip band. Phil Mag 2013;93:3809–20.
- [18] Essmann U, Gösele U, Mughrabi H. A model of extrusions and intrusions in fatigued metals. I. Point-defect production and the growth of extrusions. Phil Mag 1981;44:405–26.
- [19] Polák J. On the role of point defects in fatigue crack initiation. Mater Sci Eng 1987;92:71–80.
- [20] Polák J, Sauzay M. Growth of extrusions in localized cyclic plastic straining. Mater Sci Eng A 2009;500:122–9.
- [21] Polák J, Man J. Mechanisms of extrusion and intrusion formation in fatigued crystalline materials. Mater Sci Eng A 2014;596:15–24.

- [22] Serre I, Salazar D, Vogt J-B. LCF mechanisms of the 25Cr7Ni0.25N duplex stainless steel investigated by atomic force microscopy. *Mater Test* 2009;51:365–9.
- [23] Man J, Klapetek P, Man O, Weidner A, Obrtlík K, Polák J. Extrusions and intrusions in fatigued metals. Part 2. AFM and EBSD study of the early growth of extrusions and intrusions in 316L steel fatigued at room temperature. *Phil Mag* 2009;89:1337–72.
- [24] Hamada AS, Karjalainen LP, Puustinen J. Fatigue behavior of high-Mn TWIP steels. *Mater Sci Eng A* 2009;517:68–77.
- [25] Polák J, Man J, Vystavěl T, Petrevec M. The shape of extrusions and intrusions and initiation of stage I fatigue cracks. *Mater Sci Eng A* 2009;517:204–11.
- [26] Man J, Vystavěl T, Weidner A, Kuběna I, Petrevec M, Kruml T, et al. Study of cyclic strain localization and fatigue crack initiation using FIB technique. *Int J Fatigue* 2012;39:44–53.
- [27] Wang Y, Meletis EI, Huang H. Quantitative study of surface roughness evolution during low-cycle fatigue of 316L stainless steel using Scanning Whitelight Interferometric (SWLI) microscopy. *Int J Fatigue* 2013;48:280–8.
- [28] Polák J, Kuběna I, Man J. The shape of early persistent slip markings in fatigued 316L steel. *Mater Sci Eng A* 2013;564:8–12.
- [29] Mu P, Aubin V, Alvarez-Armas I, Armas A. Influence of the crystalline orientations on microcrack initiation in low-cycle fatigue. *Mater Sci Eng A* 2013;573:45–53.
- [30] Cottrell AH, Hull D. Extrusion and intrusion by cyclic slip in copper. *Proc Roy Soc A* 1957;242:211–3.
- [31] Hull D. Surface structure of slip bands on copper fatigued at 293°, 90°, 20°, and 4.2°K. *J Inst Metals* 1957–58;86:425–30.
- [32] Kwon IB, Fine ME, Weertman J. Fatigue damage in copper single crystals at room and cryogenic temperatures. *Acta Mater* 1989;37:2937–46.
- [33] Kwon IB, Fine ME, Weertman J. Microstructural studies on the initiation and growth of small fatigue cracks at 298, 77 and 4.2 K in polycrystalline copper. *Acta Mater* 1989;37:2927–36.
- [34] Basinski ZS, Basinski SJ. Copper single crystal PSB morphology between 4.2 and 350 K. *Acta Metall* 1989;37:3263–73.
- [35] Mughrabi H, Bayerlein M, Wang R. Direct measurement of the rate of extrusion growth in fatigued copper mono- and polycrystals. In: Brandon DG, Chaim R, Rosen A, editors. *Proc. of the ninth int. conf. on strength of metals and alloys (ICSMA 9)*, Vol. 2. London: Freund Publishing Comp. Ltd.; 1991. p. 879–86.
- [36] Bayerlein M, Mughrabi H. The formation of either tongue- or ribbon-like extrusions in fatigued copper polycrystals. *Acta Metall Mater* 1991;39:1645–50.
- [37] Man J, Obrtlík K, Polák J. Study of surface relief evolution in fatigued 316L austenitic stainless steel by AFM. *Mater Sci Eng A* 2003;351:123–32.
- [38] Man J, Valtr M, Weidner A, Petrevec M, Obrtlík K, Polák J. AFM study of surface relief evolution in 316L steel fatigued at low and high temperatures. *Proc Eng* 2010;2:1625–33.
- [39] Polák J, Petrevec M, Man J. Cyclic stress in 316L austenitic stainless steel at low temperatures. *Mater Sci Forum* 2008;567–568:401–4.
- [40] Polák J, Man J, Obrtlík K. AFM evidence of surface relief formation and models of fatigue crack nucleation. *Int J Fatigue* 2003;25:1027–36.
- [41] Lukáš P, Klesnil M. Dislocation structures in fatigued Cu–Zn single crystals. *Phys Stat Sol* 1970;37:833–42.
- [42] Wang Z, Gong B, Wang ZG. Cyclic deformation behavior of Cu–30 wt% Zn single crystals oriented for single slip. I. Cyclic deformation response and slip band behavior. *Acta Mater* 1999;47:307–15.
- [43] Mughrabi H, Ackermann F, Hertz K. Persistent slipbands in fatigued face-centered and body-centered cubic metals. In: Fong JT, editor. *Fatigue mechanisms*, ASTM STP 675. Philadelphia: American Society for Testing and Materials; 1979. p. 69–105.
- [44] Laird C, Charsley P, Mughrabi H. Low energy dislocation structures produced by cyclic deformation. *Mater Sci Eng* 1986;81:433–50.
- [45] Johnson EW, Johnson HH. Imperfection density of fatigued and annealed copper via electrical resistivity measurements. *Trans Metall Soc AIME* 1965;233:1333–9.
- [46] Polák J. Electrical resistivity of cyclically deformed copper. *Czech J Phys B* 1969;19:315–22.
- [47] Polák J. Study of fatigue in copper by resistometric method. *Kovove Mater* 1973;11:547–63 (in Czech).
- [48] Basinski ZS, Basinski SJ. Electrical resistivity of fatigued copper crystals. *Acta Metall* 1989;37:3275–81.
- [49] Polák J, Lepistö T, Kettunen P. Surface topography and crack initiation in emerging persistent slip bands in copper single crystals. *Mater Sci Eng* 1985;74:85–91.
- [50] Dimitrov O, Dimitrov C. Defect recovery in irradiated high-purity austenitic Fe–Cr–Ni alloys: activation energies and dependence on initial defect concentration. *J Nucl Mater* 1982;105:39–47.
- [51] Obrtlík K, Kruml T, Polák J. Dislocation structures in 316L stainless steel cycled with plastic strain amplitudes over a wide interval. *Mater Sci Eng A* 1994;187:1–9.
- [52] Ma B-T, Laird C. Overview of fatigue behavior in copper single crystals – I. Surface morphology and stage I crack initiation sites for tests at constant strain amplitude. *Acta Metall* 1989;37:325–36.
- [53] Polák J, Man J. Fatigue crack initiation – the role of point defects. *Int J Fatigue* 2014;65:18–27.